

# Time-domain inspiral templates for spinning compact binaries in quasi-circular orbits described by their orbital angular momenta

A Gupta<sup>1</sup> & A Gopakumar<sup>1</sup>

<sup>1</sup> Department of Astronomy and Astrophysics, Tata Institute of Fundamental Research, Mumbai 400005, India

E-mail: arg@tifr.res.in, gopu@tifr.res.in

## Abstract.

We present a prescription to compute the time-domain gravitational wave (GW) polarization states associated with spinning compact binaries inspiraling along quasi-circular orbits. We invoke the orbital angular momentum  $\mathbf{L}$  rather than its Newtonian counterpart  $\mathbf{L}_N$  to describe the binary orbits while the two spin vectors are freely specified in an inertial frame associated with the initial direction of the total angular momentum. We show that the use of  $\mathbf{L}$  to describe the orbits leads to additional 1.5PN order amplitude contributions to the two GW polarization states compared to the  $\mathbf{L}_N$ -based approach and discuss few implications of our approach. Further, we provide a plausible prescription for GW phasing based on certain theoretical considerations and which may be treated as the natural circular limit to GW phasing for spinning compact binaries in inspiraling eccentric orbits [Gopakumar A and Schäfer G 2011 *Phys. Rev. D* **84** 124007].

PACS numbers: 04.30.-w, 04.25.Nx, 97.60.Lf, 98.35.Jk

Submitted to: *Class. Quantum Grav.*

## 1. Introduction

Gravitational waves from coalescing compact binaries containing at least one spinning component are promising GW sources for the second-generation laser interferometric detectors like advanced LIGO, Virgo and KAGRA [1, 2, 3]. The detection of GWs from such binaries and the subsequent source characterization crucially depend on accurately modeling temporally evolving GW polarization states,  $h_+(t)$  and  $h_\times(t)$ , from such binaries during their inspiral phase [4]. Fortunately, inspiral phase of the compact binaries can be accurately described by the post-Newtonian (PN) approximation to general relativity [5]. At present,  $h_+(t)$  and  $h_\times(t)$  associated with non-spinning compact binaries inspiraling along quasi-circular orbits have GW phase evolution accurate to 3.5PN order and amplitude corrections that are 3PN accurate [6, 7, 8]. Recall that the 3.5PN and 3PN orders correspond to corrections that are accurate to relative orders  $(v/c)^7$  and  $(v/c)^6$  beyond the ‘Newtonian’ estimates, where  $v$  and  $c$  are the orbital and light speeds, respectively.

Obviously, GWs from compact binaries containing Kerr BHs should be extracted from the noisy interferometric data by employing temporally evolving  $h_+(t)$  and  $h_\times(t)$  that incorporate spin effects very accurately and the dominant spin effect arises due to the general relativistic spin-orbit coupling [9]. In the PN terminology, the spin-orbit coupling enters the orbital dynamics formally at 1PN order and for moderate spin values  $v_{\text{spin}} \ll c$ , the coupling numerically appears at the  $\mathcal{O}(1/c^4)$  level or at the 2PN order [10]. However, for  $v_{\text{spin}} \sim c$ , the spin-orbit contributions manifest at slightly more dominant  $\mathcal{O}(1/c^3)$  level or the 1.5PN order [9]. We define the spin of a compact object as  $\mathbf{S} = G m_{\text{co}}^2 \chi \mathbf{s}/c$ , where  $m_{\text{co}}, \chi$  and  $\mathbf{s}$  are its mass, Kerr parameter and a unit vector along  $\mathbf{S}$ , respectively. This definition implies that for a maximally spinning Kerr BH  $\chi = 1$  and for neutron stars typical upper limit to  $\chi$  values should be  $\sim 0.4$  [11]. At present, all contributions to the GW phase evolution are available to the next-to-leading order (2.5PN order), while amplitude corrected  $h_+(t)$  and  $h_\times(t)$  are computed to 2PN order for spinning compact binaries in quasi-circular orbits [9, 12, 13, 14, 15]. Further, it is customary to employ the Newtonian orbital angular momentum  $\mathbf{L}_N = \mu \mathbf{r} \times \mathbf{v}$ , where  $\mu, \mathbf{r}$  and  $\mathbf{v}$  are the reduced mass, orbital separation and velocity, respectively, to specify these quasi-circular orbits.

In this paper we provide a prescription to generate the time-domain amplitude corrected  $h_+(t)$  and  $h_\times(t)$  for spinning compact binaries inspiraling along quasi-circular orbits, described by their orbital angular momenta. Note that the amplitude corrected  $h_+(t)$  and  $h_\times(t)$  refer to GW polarization states that are PN-accurate both in its amplitude and phase. We begin by describing our GW phasing approach while considering spinning compact binaries influenced by the leading order general relativistic spin-orbit coupling and the 2PN accurate inspiral dynamics (following the literature, we term accurate modeling of temporally evolving GW polarization states as ‘GW phasing’). We discuss, in detail, certain implications of our approach where we freely specify the two spins at the initial epoch in an inertial frame, defined by the initial direction of the total angular momentum  $\mathbf{j}_0$ . In contrast, it is customary to invoke a  $\mathbf{L}_N$ -based orbital triad to specify the two spins at the initial epoch in the literature [9, 14, 16]. Our attempt to invoke  $\mathbf{L}$  while constructing inspiral templates is motivated by the following considerations. We observe that a seminal paper that explored the inspiral dynamics of spinning compact binaries and the influences of precessional dynamics on  $h_{+,\times}(t)$  employed  $\mathbf{L}$  to describe their binary orbits [17]. Moreover, the  $\mathbf{L}$  variable naturally appears while invoking the canonical formalism of Arnowitt, Deser, and Misner to describe the dynamics of compact spinning binaries [18, 19]. We also discuss the theoretical consequence of employing the precessional equation appropriate for  $\mathbf{L}$  during the numerical evolution of  $\mathbf{L}_N$ . We show that it can lead to certain anomalous 3PN order terms in the differential equation for the orbital (and GW) phase evolution. The fact that we invoke  $\mathbf{L}$  to describe the binary orbits leads to additional 1.5PN order amplitude corrections to  $h_+(t)$  and  $h_\times(t)$  compared to equations (A2) and (A3) in [14] that provide amplitude corrected GW polarization states while employing  $\mathbf{L}_N$  to describe the binary orbits. We provide the reason for the presence of these additional terms in our approach and obtain explicit expressions for them. This implies that these contributions along with equations (A2) and (A3) in [14] would lead to the fully 1.5PN accurate amplitude corrected  $h_+(t)$  and  $h_\times(t)$  in our approach, provided their  $\iota$  and  $\alpha$  variables specify the orientation of  $\mathbf{L}$  rather than  $\mathbf{L}_N$  (see figure 1 in [14]).

Let us emphasize that it is equally valid to invoke either  $\mathbf{L}$  or  $\mathbf{L}_N$  to describe orbits associated with spinning compact binaries. This implies that the equations (A2)

and (A3) in [14] indeed provide the fully 1.5PN accurate amplitude corrected  $h_+(t)$  and  $h_\times(t)$  for spinning compact binaries in quasi-circular orbits, described by  $\mathbf{L}_N$ . It will be desirable to employ the appropriate differential equation for  $\mathbf{L}_N$ , namely our equation (24), in order to make sure that there are no anomalous 3PN order terms in the differential equation for the orbital phase evolution. We note that the recent detailed PN computations should allow one, in principle, to write down a PN-accurate differential equation for the orbital phase while incorporating the 3.5PN order next-to-next leading order spin-orbit interactions and 4PN order spin-spin interactions [20, 21, 22]. However, our GW phase evolution is identical to what is provided in [14] as both these investigations incorporate only the dominant 1.5PN accurate spin-orbit effects.

Subsequently, we introduce a plausible prescription to do GW phasing influenced by the following few theoretical considerations. These include our observation that  $\omega_{\text{orb}}$  naturally exists in a  $\mathbf{L}_N$ -based orbital triad such that  $\omega_{\text{orb}} \equiv \dot{\mathbf{n}} \cdot \boldsymbol{\lambda}$ , where  $\boldsymbol{\lambda} = \mathbf{l} \times \mathbf{n}$  and  $\dot{\mathbf{n}} = d\mathbf{n}/dt$ :  $\mathbf{n}$  and  $\mathbf{l}$  are unit vectors along  $\mathbf{r}$  and  $\mathbf{L}_N$ , respectively. Further, it turns out that  $\int \omega_{\text{orb}}(t') dt'$  (and its multiples) can provide GW phase evolutions for spinning binaries only when orbital inclinations are tiny as evident from equations (3.16) and (3.17) in [14]. Therefore, we provide a prescription that allows us to impose the effects of gravitational radiation reaction on the conservative evolution of various angles present in the expressions for  $h_+(t)$  and  $h_\times(t)$  without invoking  $\omega_{\text{orb}}$ . This approach may be treated as the natural circular limit of GW phasing for compact binaries in inspiraling eccentric orbits, detailed in [23], as this prescription also requires the orbital energy as the PN expansion parameter. The above approach looks similar to Taylor-Et approximant, introduced in [24] for non-precessing binaries, which turned out to be undesirable for data analysis purposes involving GWs from non-spinning compact binaries as detailed in [25]. Further investigations will be required to probe the physical implications of our theoretical arguments and it should not be treated as an alternative to the orbital-like frequency  $\omega_{\text{orb}}$  based approach. At present, our aim is to point out the theoretical subtleties involved in the phasing.

The paper is organized as follows. In section 2, we provide details of performing GW phasing for spinning compact binaries described by  $\mathbf{L}$ , list features of our approach and probe the consequence of employing precessional equation of  $\mathbf{L}$  while numerically evolving  $\mathbf{L}_N$ . An approach that does not require  $\omega_{\text{orb}}$  while computing the time-domain  $h_+(t)$  and  $h_\times(t)$  for spinning compact binaries is detailed in section 3, while section 4 provides our conclusions and possible extensions.

## 2. GW phasing for spinning binaries in quasi-circular orbits specified by $\mathbf{L}$ and an orbital-like frequency

We begin by listing formulae required to obtain amplitude corrected GW polarization states from the transverse–traceless (TT) part of the radiation field,  $h_{ij}^{\text{TT}}$ :

$$h_+ = \frac{1}{2} (p_i p_j - q_i q_j) h_{ij}^{\text{TT}}, \quad (1a)$$

$$h_\times = \frac{1}{2} (p_i q_j + p_j q_i) h_{ij}^{\text{TT}}, \quad (1b)$$

where the orthogonal unit vectors  $\mathbf{p}$  and  $\mathbf{q}$  live in a plane transverse to the line-of-sight unit vector  $\mathbf{N}$  defined as  $\mathbf{N} = \mathbf{R}'/R'$ , where  $R' = |\mathbf{R}'|$  is the radial distance from the observer to the binary (see figure 1). Following [14], the vectors  $\mathbf{p}$  and  $\mathbf{q}$

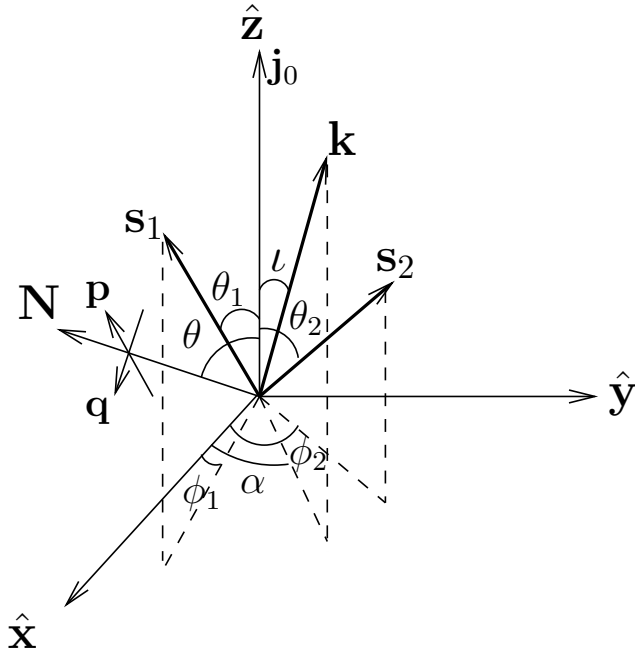


**Figure 1.** The Cartesian coordinate system where the  $\hat{z}$  axis points along  $\mathbf{j}_0$ , the direction of total angular momentum at the initial epoch. We display angles that characterize the orbital and spin angular momentum vectors, denoted by  $\mathbf{k}$ ,  $\mathbf{s}_1$  and  $\mathbf{s}_2$ , while the line of sight vector  $\mathbf{N}$  is in the  $x-z$  plane. The dashed lines depict projections of various vectors on the  $x-y$  plane. This inertial Cartesian coordinate system is also known as the source frame in the literature.

are defined with the help of  $\mathbf{N}$  and  $\mathbf{j}_0$ , a unit vector along the direction of the total angular momentum at the initial epoch, as

$$\mathbf{p} = \frac{\mathbf{N} \times \mathbf{j}_0}{|\mathbf{N} \times \mathbf{j}_0|}, \quad (2a)$$

$$\mathbf{q} = \mathbf{N} \times \mathbf{p}. \quad (2b)$$

Amplitude corrected PN-accurate expressions for  $h_+(t)$  and  $h_\times(t)$  originate from  $h_{ij}^{\text{TT}}$  which can be expressed as a Taylor series in terms of  $v/c$  for binaries in quasi-circular orbits. The dominant contribution to  $h_{ij}^{\text{TT}}$  arises from the time varying Newtonian order quadrupole moment of the binary and is given by

$$h_{km}^{\text{TT}}|_{\text{Q}} = \frac{4G\mu}{c^4 R'} \mathcal{P}_{ijkm}(\mathbf{N}) \left( v_{ij} - \frac{Gm}{r} n_{ij} \right), \quad (3)$$

where  $\mathcal{P}_{ijkm}(\mathbf{N})$  is the transverse traceless projection operator projecting vectors normal to  $\mathbf{N}$ ,  $\mu$  being the reduced mass ( $\mu = m_1 m_2 / m$ ) while  $m$  denotes the total mass,  $m = m_1 + m_2$ . In the above equation, we denoted the components of  $\mathbf{n} = \mathbf{r}/r$  and the velocity vector  $\mathbf{v} = d\mathbf{r}/dt$  by  $n_i$  and  $v_i$  and defined  $v_{ij} := v_i v_j$ , and  $n_{ij} := n_i n_j$ .

The two resulting GW polarization states are

$$h_+|_Q = \frac{2G\mu}{c^4 R'} \left\{ (\mathbf{p} \cdot \mathbf{v})^2 - (\mathbf{q} \cdot \mathbf{v})^2 - \frac{Gm}{r} [(\mathbf{p} \cdot \mathbf{n})^2 - (\mathbf{q} \cdot \mathbf{n})^2] \right\}, \quad (4a)$$

$$h_\times|_Q = \frac{4G\mu}{c^4 R'} \left[ (\mathbf{p} \cdot \mathbf{v})(\mathbf{q} \cdot \mathbf{v}) - \frac{Gm}{r} (\mathbf{p} \cdot \mathbf{n})(\mathbf{q} \cdot \mathbf{n}) \right]. \quad (4b)$$

Clearly, these expressions are for compact binaries in general orbits and their circular versions are obtained by using  $v^2 = Gm/r$ , after evaluating above dot products. The expressions for  $h_+(t)$  and  $h_\times(t)$  suitable for constructing inspiral templates for spinning compact binaries inspiraling along quasi-circular orbits can be obtained with the help of following few steps. In the first step, we express  $\mathbf{r}$  and  $\mathbf{v}$  in the inertial frame  $(\hat{x}, \hat{y}, \hat{z})$ , where  $\hat{z}$  points along  $\mathbf{j}_0$ , with the help of the three Eulerian angles  $\Phi, \alpha$  and  $\iota$  defined in the inertial frame. The resulting expression for  $\mathbf{r}$  reads

$$\mathbf{r} = r\mathbf{n}, \text{ where} \quad (5a)$$

$$\mathbf{n} = (-\sin \alpha \cos \Phi - \cos \iota \cos \alpha \sin \Phi, \cos \alpha \cos \Phi - \cos \iota \sin \alpha \sin \Phi, \sin \iota \sin \Phi), \quad (5b)$$

and the velocity vector becomes  $\mathbf{v} = d\mathbf{r}/dt = r d\mathbf{n}(\Phi, \iota, \alpha)/dt$  for circular orbits [26]. For our purpose it is convenient to represent various vectors present in equations (4) in the comoving frame defined by the triad  $(\mathbf{n}, \boldsymbol{\xi} = \mathbf{k} \times \mathbf{n}, \mathbf{k})$ , where  $\mathbf{k}$  is the unit vector along  $\mathbf{L}$ . This is easily achieved with the help of three rotations involving the three Eulerian angles appearing in the expression for  $\mathbf{r}$  [10, 26]. The components of  $\mathbf{r}, \mathbf{v}, \mathbf{p}, \mathbf{q}$  and  $\mathbf{N}$  in the comoving frame are given by

$$\mathbf{r} = r\mathbf{n}, \quad (6a)$$

$$\mathbf{v} = r \left( \frac{d\Phi}{dt} + \frac{d\alpha}{dt} \cos \iota \right) \boldsymbol{\xi} + r \left( \frac{d\iota}{dt} \sin \Phi - \sin \iota \cos \Phi \frac{d\alpha}{dt} \right) \mathbf{k}, \quad (6b)$$

$$\mathbf{p} = (\sin \Phi \cos \iota \sin \alpha - \cos \Phi \cos \alpha) \mathbf{n} + (\sin \Phi \cos \alpha + \cos \Phi \cos \iota \sin \alpha) \boldsymbol{\xi} - \sin \iota \sin \alpha \mathbf{k}, \quad (6c)$$

$$\mathbf{q} = (-\sin \Phi \sin \iota \sin \theta - \cos \Phi \sin \alpha \cos \theta - \sin \Phi \cos \iota \cos \alpha \cos \theta) \mathbf{n} + (-\cos \Phi \cos \iota \cos \alpha \cos \theta - \cos \Phi \sin \iota \sin \theta + \sin \Phi \sin \alpha \cos \theta) \boldsymbol{\xi} + (\sin \iota \cos \alpha \cos \theta - \cos \iota \sin \theta) \mathbf{k}, \quad (6d)$$

$$\mathbf{N} = (-\cos \Phi \sin \alpha \sin \theta - \sin \Phi \cos \iota \cos \alpha \sin \theta + \sin \Phi \sin \iota \cos \theta) \mathbf{n} + (\sin \Phi \sin \alpha \sin \theta - \cos \Phi \cos \iota \cos \alpha \sin \theta + \cos \Phi \sin \iota \cos \theta) \boldsymbol{\xi} + (\sin \iota \cos \alpha \sin \theta + \cos \iota \cos \theta) \mathbf{k}, \quad (6e)$$

where we used equations (2) for  $\mathbf{p}$  and  $\mathbf{q}$  and let  $\mathbf{j}_0 = (0, 0, 1)$  and  $\mathbf{N} = (\sin \theta, 0, \cos \theta)$  in the inertial frame as shown in figure 1. The vectors defining the comoving frame, namely  $\mathbf{n}, \boldsymbol{\xi}$  and  $\mathbf{k}$ , have following components in the inertial frame

$$\boldsymbol{\xi} = (\sin \alpha \sin \Phi - \cos \iota \cos \alpha \cos \Phi, -\cos \alpha \sin \Phi - \cos \iota \sin \alpha \cos \Phi, \sin \iota \cos \Phi), \quad (7a)$$

$$\mathbf{k} = (\sin \iota \cos \alpha, \sin \iota \sin \alpha, \cos \iota), \quad (7b)$$

while  $\mathbf{n}$  is specified by equation (5b) such that  $\Phi$  measures the orbital phase from the direction of ascending node in the  $x - y$  plane.

It is now fairly straightforward to obtain explicit expressions for  $h_{+, \times}|_Q$  in terms of various angular variables with the help of equations (6) and the resulting expressions read

$$\begin{aligned}
h_{+}|_Q = \frac{2G\mu v^2}{c^4 R'} & \left\{ \left( \frac{3}{2} \cos^2 \iota - \frac{3}{2} \right) (1 - C_\theta^2) \cos 2\Phi \right. \\
& - (1 + \cos \iota) S_\theta C_\theta \sin \iota \cos(2\Phi + \alpha) \\
& - \frac{1}{4} (\cos^2 \iota + 2 \cos \iota + 1) (1 + C_\theta^2) \cos(2\alpha + 2\Phi) \\
& - \frac{1}{4} (\cos^2 \iota - 2 \cos \iota + 1) (1 + C_\theta^2) \cos(2\alpha - 2\Phi) \\
& - S_\theta C_\theta \sin \iota \cos \iota \cos(\alpha - 2\Phi) \\
& \left. + S_\theta C_\theta \sin \iota \cos(\alpha - 2\Phi) \right\}, \tag{8a}
\end{aligned}$$

$$\begin{aligned}
h_{\times}|_Q = \frac{2G\mu v^2}{c^4 R'} & \left\{ (1 - \cos \iota) S_\theta \sin \iota \sin(\alpha - 2\Phi) \right. \\
& - (1 + \cos \iota) S_\theta \sin \iota \sin(\alpha + 2\Phi) \\
& - \frac{1}{2} (1 + 2 \cos \iota + \cos^2 \iota) C_\theta \sin(2\alpha + 2\Phi) \\
& \left. - \frac{1}{2} (1 - 2 \cos \iota + \cos^2 \iota) C_\theta \sin(2\alpha - 2\Phi) \right\}, \tag{8b}
\end{aligned}$$

where  $v^2/c^2 = (Gm\dot{\Phi}/c^3)^{2/3}$  while  $S_\theta$  and  $C_\theta$  stand for  $\sin \theta$  and  $\cos \theta$ , respectively. To obtain above the expressions from equation (4a) and (4b), we used the Newtonian accurate relation,  $v^2 = r^2 \dot{\Phi}^2 = Gm/r$  arising from equation (6b) for  $\mathbf{v}$  and let  $(r\dot{\Phi})/c = (Gm\dot{\Phi}/c^3)^{1/3}$ .

GW phasing for inspiraling binaries containing spinning compact objects is performed by first prescribing differential equations that provide precessional (conservative) evolution for various Eulerian angles present in the expressions for  $h_{+, \times}(t)$ . Thereafter, one imposes the effect of radiation damping on these conservative evolutions. We begin by prescribing the differential equation for  $\Phi$  based on the following considerations [9]. With the help of equation (6b) for  $\mathbf{v}$ , we write down the following expression for  $v^2$  to the desired 1.5 PN order

$$v^2 = r^2 \dot{\Phi}^2 + 2r^2 \dot{\Phi} \dot{\alpha} \cos \iota, \tag{9}$$

and this leads to  $v = r(\dot{\Phi} + \cos \iota \dot{\alpha})$ . Invoking an orbital-like frequency  $\omega_{\text{orb}} \equiv v/r$ , we write

$$\dot{\Phi} = \omega_{\text{orb}} - \cos \iota \dot{\alpha}. \tag{10}$$

It is convenient to introduce a dimensionless parameter  $x \equiv (Gm\omega_{\text{orb}}/c^3)^{2/3}$ , allowing us to obtain following equation for the conservative evolution of  $\Phi$ :

$$\dot{\Phi} = \frac{x^{3/2}}{(Gm/c^3)} - \cos \iota \dot{\alpha}. \tag{11}$$

The conservative evolution of  $\alpha$  and  $\iota$  may be extracted from the precessional equations for  $\mathbf{k}$  as  $\alpha$  and  $\iota$  specify  $\mathbf{k}$  in the inertial frame. The structure of  $\dot{\mathbf{k}}$  demands us to

solve (numerically) precessional equation for  $\mathbf{k}$  together with those for  $\mathbf{s}_1$  and  $\mathbf{s}_2$ . The relevant equations, extractable from [9, 13], read

$$\dot{\mathbf{k}} = \frac{c^3}{Gm} x^3 \left\{ \delta_1 q \chi_1 (\mathbf{s}_1 \times \mathbf{k}) + \frac{\delta_2}{q} \chi_2 (\mathbf{s}_2 \times \mathbf{k}) \right\}, \quad (12a)$$

$$\dot{\mathbf{s}}_1 = \frac{c^3}{Gm} x^{5/2} \delta_1 (\mathbf{k} \times \mathbf{s}_1), \quad (12b)$$

$$\dot{\mathbf{s}}_2 = \frac{c^3}{Gm} x^{5/2} \delta_2 (\mathbf{k} \times \mathbf{s}_2), \quad (12c)$$

where  $q = m_1/m_2$  and the Kerr parameters  $\chi_n$  specify the spin vectors by  $\mathbf{S}_n = G m_n^2 \chi_n \mathbf{s}_n/c$ , where the subscript  $n$  can take values 1 or 2. The symmetric mass ratio  $\eta = \mu/m$  is required to define the quantities  $\delta_1$  and  $\delta_2$  as

$$\delta_1 = \frac{\eta}{2} + \frac{3}{4} (1 - \sqrt{1 - 4\eta}), \quad (13a)$$

$$\delta_2 = \frac{\eta}{2} + \frac{3}{4} (1 + \sqrt{1 - 4\eta}). \quad (13b)$$

We note that the equations (12) provide precessional dynamics due to the dominant order spin-orbit coupling. Further, for the purpose of numerical integration we specify the components of  $\mathbf{s}_1$  and  $\mathbf{s}_2$  in the inertial frame associated with  $\mathbf{j}_0$  as

$$\mathbf{s}_1 = (\sin \theta_1 \cos \phi_1, \sin \theta_1 \sin \phi_1, \cos \theta_1), \quad (14a)$$

$$\mathbf{s}_2 = (\sin \theta_2 \cos \phi_2, \sin \theta_2 \sin \phi_2, \cos \theta_2), \quad (14b)$$

as displayed in figure 1.

We are now in a position to incorporate the effect of gravitational radiation damping and this is achieved by imposing secular evolution of  $x$  in equations (11) and (12). In this paper, we employ the 2PN-accurate expression for  $\dot{x}$  that requires the usual energy balance argument and available in [13]:

$$\begin{aligned} \frac{dx}{dt} = & \frac{64}{5} \frac{c^3}{Gm} \eta x^5 \left\{ 1 + x \left[ -\frac{743}{336} - \frac{11\eta}{4} \right] + 4\pi x^{3/2} \right. \\ & + \frac{x^{3/2}}{12} \left[ (-188 X_1 + 75\sqrt{1 - 4\eta}) X_1 \chi_1 (\mathbf{s}_1 \cdot \mathbf{k}) \right. \\ & \left. \left. + (-188 X_2 - 75\sqrt{1 - 4\eta}) X_2 \chi_2 (\mathbf{s}_2 \cdot \mathbf{k}) \right] \right. \\ & \left. + x^2 \left[ \frac{34103}{18144} + \frac{13661}{2016} \eta + \frac{59}{18} \eta^2 \right] \right\}, \quad (15) \end{aligned}$$

where  $X_1 = m_1/m$  and  $X_2 = m_2/m$ .

We propose to solve together equations (11), (12) and (15) numerically, while invoking the Cartesian components of the precessional equations and specifying the spin vectors in the inertial frame defined by  $\mathbf{j}_0$ . Naturally, we need to specify initial conditions for the Cartesian components of  $\mathbf{k}$ ,  $\mathbf{s}_1$  and  $\mathbf{s}_2$  in the inertial frame. These components for  $\mathbf{s}_1$  and  $\mathbf{s}_2$  are obtained with the help of equations (14) by specifying all possible initial values for  $(\theta_1, \phi_1)$  and  $(\theta_2, \phi_2)$ . The fact that we align the total angular momentum along  $z$ -axis at the initial epoch allows us to equate the  $x$  and  $y$

components of  $\mathbf{J} = \mathbf{L} + \mathbf{S}_1 + \mathbf{S}_2$  at the initial instant to zero. This results in the following expressions to estimate initial values of the Cartesian components of  $\mathbf{k}$

$$k_{x,0} = -\frac{G m^2}{c L_{2\text{PN}}(x_0)} \{X_1^2 \chi_1 \sin \theta_{10} \cos \phi_{10} + X_2^2 \chi_2 \sin \theta_{20} \cos \phi_{20}\}, \quad (16a)$$

$$k_{y,0} = -\frac{G m^2}{c L_{2\text{PN}}(x_0)} \{X_1^2 \chi_1 \sin \theta_{10} \sin \phi_{10} + X_2^2 \chi_2 \sin \theta_{20} \sin \phi_{20}\}, \quad (16b)$$

where  $\theta_{10}$ ,  $\theta_{20}$ ,  $\phi_{10}$  and  $\phi_{20}$  are the initial values of  $\theta_1, \theta_2, \phi_1$  and  $\phi_2$ , respectively while  $L_{2\text{PN}}(x_0)$  denotes the value of the 2PN accurate orbital angular momentum at  $x = x_0 = x(t_0)$ . The relevant analytic expression for  $L_{2\text{PN}}$  is given by [13]

$$\mathbf{L}_{2\text{PN}} = \frac{G m^2 \eta}{c} x^{-1/2} \left\{ 1 + x \left[ \frac{3}{2} + \frac{\eta}{6} \right] + x^2 \left[ \frac{27}{8} - \frac{19\eta}{8} + \frac{\eta^2}{24} \right] \right\} \mathbf{k} \quad (17)$$

and we would like to note that the above estimates for  $k_{x,0}$  and  $k_{y,0}$  do not change substantially even if we drop PN corrections in  $\mathbf{L}_{2\text{PN}}$ . The initial values for  $\alpha$  and  $\iota$  are obtained, as expected, by equating the above expressions for  $k_{x,0}$  and  $k_{y,0}$  to  $\sin \iota \cos \alpha$  and  $\sin \iota \sin \alpha$ , respectively, and numerically solving these coupled equations. In our numerical runs, we select those solutions that provide positive  $\iota$  values at the initial epoch. The bounding values for  $x$  are given by  $x_0 = 2.9 \times 10^{-4} (m' \omega_0)^{2/3}$  and  $x_f = 1/6$ , where  $m'$  is the total mass of the binary in solar units and let  $\omega_0 = 10 \pi$  Hz as customary for aLIGO and we choose the initial phase to be zero ( $\Phi_0 = 0$ ). Finally, we note that the values of  $\alpha$  and  $\iota$  at every step of our numerical runs are obtained from the Cartesian components of  $\mathbf{k}$  by  $\alpha = \tan^{-1}(k_y/k_x)$  and  $\iota = \cos^{-1}(k_z)$ .

We are now in a position to plot the temporally evolving  $h_{+, \times} |_{\text{Q}}(t)$  for inspiraling compact binaries described by equations (8). In figures 2 and 3, we plot  $\iota(t)$  and  $h_{+, \times} |_{\text{Q}}(t)$  for few spin configurations and two mass ratios ( $q = 1$  and 4) in the aLIGO frequency window for maximally spinning BH binaries. The choice of  $m = 50 M_\odot$  allows us to explore the combined effects of precessional and reactive orbital dynamics in short time windows spanning around  $\sim 10$  seconds for both mass ratios. The spin configurations are chosen so that the more massive BH spin orientations vary from relatively smaller to larger values from  $\mathbf{j}_0$ .

Clearly, the plots in figure 2 do not show any amplitude modulations and additional numerical runs indicate similar behavior even for extreme spin configurations. This is due to the fact that for equal mass binaries  $|\mathbf{L}| \gg |\mathbf{S}|$ , where  $\mathbf{S} = \mathbf{S}_1 + \mathbf{S}_2$ , throughout the inspiral leading to tiny modulations [9, 17]. This leads to slow reactive evolutions of  $\iota$  in addition to low initial values for  $\iota$ , prescribed by equations (16), for equal mass binaries. The slower variations for  $\iota$  may also be attributed to our observation that  $\mathbf{k} \cdot \mathbf{S}_{\text{eff}}$ , where  $\mathbf{S}_{\text{eff}} = \delta_1 \mathbf{S}_1 + \delta_2 \mathbf{S}_2$ , remains a constant during the reactive evolution for equal mass binaries. We recall that the conservation of  $\mathbf{k} \cdot \mathbf{S}_{\text{eff}}$  allowed the derivation of certain Keplerian type parametric solution to the underlying dynamics in [26].

The plots in figure 3 depict temporal variations in  $\iota, h_{\times} |_{\text{Q}}$  and  $h_{+} |_{\text{Q}}$  for unequal mass maximally spinning BH binaries. We clearly observe amplitude modulations, for spin-configurations B and C, where the dominant spin is misaligned from  $\mathbf{j}_0$  by  $60^\circ$  and  $120^\circ$ , respectively. The comparatively higher and faster secular variations in  $\iota$  at the later stages of inspiral can be attributed to the fact that the spin angular



momentum of the more massive BH dominates over the orbital angular momentum during this stage. This is consistent with the deduction of [17] that pointed out faster  $\iota$  variations for spin angular momentum dominated binaries. However, the differences in  $\iota$  evolutions, evident between Spin-B and Spin-C configurations in figure 3, prompted us to include variations in  $\mathbf{k} \cdot \mathbf{S}_{\text{eff}}$  also contributing to the way  $\iota$  evolves. This is because the spin angular momentum starts dominating both these binaries at the same epoch during the late inspiral though we observe different  $\iota$  evolutions. Further, such binaries have relatively larger initial values for  $\iota$  compared to their equal mass counterparts in addition to faster secular variations in  $\iota$ . These effects clearly contribute to the observed amplitude modulations in  $h_{+, \times}|_Q(t)$ .

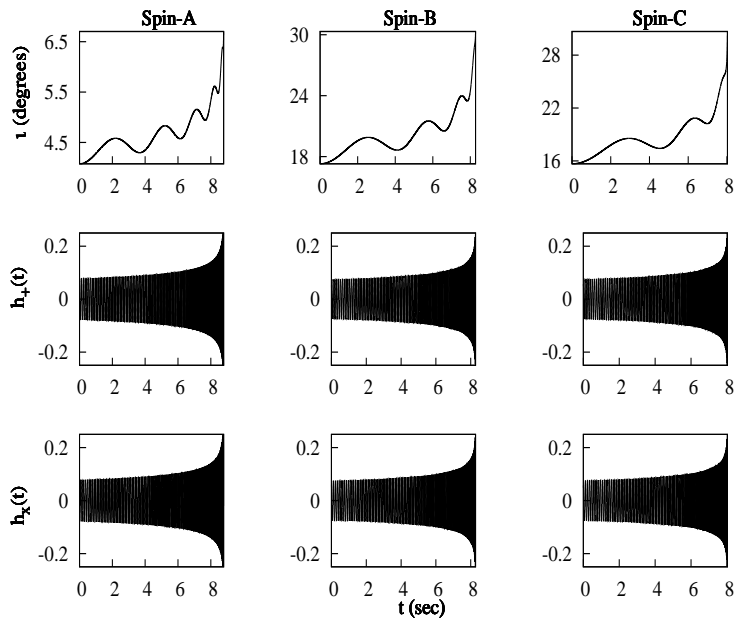


**Figure 2.** Plots showing temporally evolving  $\iota(t)$ , scaled  $h_{+}|_Q(t)$  and  $h_{\times}|_Q(t)$  for maximally spinning compact binaries ( $q = 1, m = 50M_{\odot}$ ). The three initial spin configurations are denoted by Spin-A:  $\{\theta_{10} = \pi/6, \phi_{10} = \pi/4, \theta_{20} = \pi/6, \phi_{20} = \pi\}$ , Spin-B:  $\{\theta_{10} = \pi/3, \phi_{10} = \pi/4, \theta_{20} = \pi/3, \phi_{20} = \pi/2\}$  and Spin-C:  $\{\theta_{10} = 2\pi/3, \phi_{10} = \pi/2, \theta_{20} = \pi/4, \phi_{20} = \pi/4\}$ , while the scaling factor is  $(2G\mu/c^2 R')$ . The theoretically prescribed initial values for  $\alpha$  and  $\iota$  are  $(-67.5^\circ, 4.1^\circ)$ ,  $(-112.5^\circ, 17.3^\circ)$  and  $(-110.1^\circ, 15.7^\circ)$ , respectively. Further, the initial angle between  $\mathbf{k}$  and  $\mathbf{s}_1$  for the above three spin configurations A, B and C are  $31.76^\circ$ ,  $76.14^\circ$  and  $134.52^\circ$ , respectively while the initial negative  $\alpha$  values, if required, may easily be converted to their positive counterparts by subtracting from  $2\pi$ .

In what follows we probe the consequence of employing  $\dot{\mathbf{L}}_N = -(\dot{\mathbf{S}}_1 + \dot{\mathbf{S}}_2)$  to numerically evolve  $\mathbf{l} = \mathbf{L}_N/|\mathbf{L}_N|$ . It turns out that it is equivalent to employing an orbital averaged expression for  $\dot{\mathbf{l}}$  [9]. Invoking an orbital averaged precessional equation for  $\mathbf{l}$  leads to an undesirable feature that the coefficient of  $\mathbf{l}$  in the expression for  $\dot{\mathbf{n}}$  in  $(\mathbf{n}, \boldsymbol{\lambda} = \mathbf{l} \times \mathbf{n}, \mathbf{l})$  frame will not, in general, vanish. To verify the above observation, let us specify these unit vectors in the inertial frame associated with  $\mathbf{j}_0$  using three

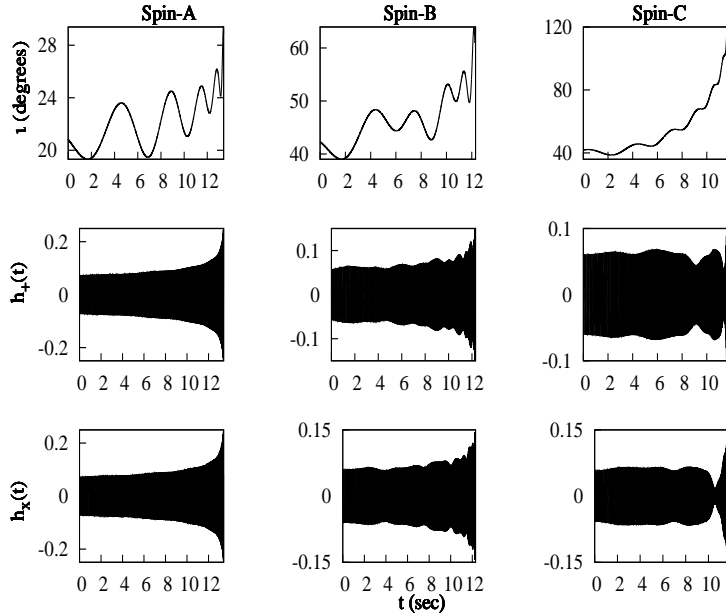


**Figure 3.** Plots, similar to figure 2, for maximally spinning unequal mass binaries ( $q = 4, m = 50M_{\odot}$ ). The prescribed initial values for  $\alpha$  and  $\iota$ , based on equations (16), for the three initial spin configurations are  $(-132.4^\circ, 20.8^\circ)$ ,  $(-132.6^\circ, 42.3^\circ)$  and  $(-91.9^\circ, 41.9^\circ)$ , respectively. The initial angle between  $\mathbf{k}$  and  $\mathbf{s}_1$  for the above three spin configurations A, B and C are  $50.82^\circ$ ,  $102.25^\circ$  and  $161.80^\circ$ , respectively. Spin induced amplitude modulations are clearly visible in spin configurations that provide substantial evolution for  $\iota$ . We observe that  $\mathbf{k} \cdot \mathbf{S}_{\text{eff}}$  vary during the inspiral and amplitude of these variations are initial spin configuration dependent.

angles  $\Phi'$ ,  $\alpha'$  and  $\iota'$  such that

$$\mathbf{n} = (-\sin \alpha' \cos \Phi' - \cos \iota' \cos \alpha' \sin \Phi', \cos \alpha' \cos \Phi' - \cos \iota' \sin \alpha' \sin \Phi', \sin \iota' \sin \Phi'), \quad (18a)$$

$$\mathbf{\lambda} = (\sin \alpha' \sin \Phi' - \cos \iota' \cos \alpha' \cos \Phi', -\cos \alpha' \sin \Phi' - \cos \iota' \sin \alpha' \cos \Phi', \sin \iota' \cos \Phi'), \quad (18b)$$

$$\mathbf{l} = (\sin \iota' \cos \alpha', \sin \iota' \sin \alpha', \cos \iota'), \quad (18c)$$

where we used *primed* variables to distinguish from the Eulerian angles present in the  $\mathbf{k}$ -based frame. It is fairly straightforward to compute the time derivative of  $\mathbf{n}$  and express it in the  $(\mathbf{n}, \mathbf{\lambda}, \mathbf{l})$  frame as

$$\frac{d\mathbf{n}}{dt} = \left( \frac{d\Phi'}{dt} + \cos \iota' \frac{d\alpha'}{dt} \right) \mathbf{\lambda} + \left( \frac{d\iota'}{dt} \sin \Phi' - \sin \iota' \cos \Phi' \frac{d\alpha'}{dt} \right) \mathbf{l}. \quad (19)$$

The fact that  $\mathbf{l} = \mathbf{n} \times \dot{\mathbf{n}} / |\mathbf{n} \times \dot{\mathbf{n}}|$  clearly demands that the coefficient of  $\mathbf{l}$  in the above equation should be zero as also noted in [14]. However, if one employs equation (12a) as the precessional equation for  $\mathbf{l}$  namely

$$\dot{\mathbf{l}} = \frac{c^3}{Gm} x^3 \left\{ \delta_1 q \chi_1 (\mathbf{s}_1 \times \mathbf{l}) + \frac{\delta_2}{q} \chi_2 (\mathbf{s}_2 \times \mathbf{l}) \right\}, \quad (20)$$

then it is possible to show with some straightforward algebra that

$$\sin \Phi' \frac{dt'}{dt} - \cos \Phi' \sin l' \frac{d\alpha'}{dt} = -\frac{c^3}{Gm} x^3 \left\{ \delta_1 q \chi_1 (\mathbf{s}_1 \cdot \boldsymbol{\lambda}) + \frac{\delta_2}{q} \chi_2 (\mathbf{s}_2 \cdot \boldsymbol{\lambda}) \right\}. \quad (21)$$

It is not very difficult to conclude that the right hand side of above expression, in general, is not zero. The above equation is obtained by employing following equations for  $dt'/dt$  and  $d\alpha'/dt$

$$\begin{aligned} \frac{dt'}{dt} = \frac{c^3}{Gm} x^3 & \left\{ [\delta_1 q \chi_1 (\mathbf{s}_1 \cdot \mathbf{n}) + \frac{\delta_2}{q} \chi_2 (\mathbf{s}_2 \cdot \mathbf{n})] \cos \Phi' \right. \\ & \left. - [\delta_1 q \chi_1 (\mathbf{s}_1 \cdot \boldsymbol{\lambda}) + \frac{\delta_2}{q} \chi_2 (\mathbf{s}_2 \cdot \boldsymbol{\lambda})] \sin \Phi' \right\}, \end{aligned} \quad (22a)$$

$$\begin{aligned} \frac{d\alpha'}{dt} \sin l' = \frac{c^3}{Gm} x^3 & \left\{ [\delta_1 q \chi_1 (\mathbf{s}_1 \cdot \boldsymbol{\lambda}) + \frac{\delta_2}{q} \chi_2 (\mathbf{s}_2 \cdot \boldsymbol{\lambda})] \cos \Phi' \right. \\ & \left. + [\delta_1 q \chi_1 (\mathbf{s}_1 \cdot \mathbf{n}) + \frac{\delta_2}{q} \chi_2 (\mathbf{s}_2 \cdot \mathbf{n})] \sin \Phi' \right\}, \end{aligned} \quad (22b)$$

and these equations easily arise from equation (18c) for  $\mathbf{l}$  and equation (20) for  $\dot{\mathbf{l}}$ .

It is possible to correct the above inconsistency by using the appropriate precessional equation for  $\mathbf{l}$  as noted in [23]. In the covariant Spin-Supplementary-Condition (SSC) pursued here [27], the precessional equation for  $\mathbf{l}$  arises from the following PN-accurate expression that connects  $\mathbf{l}$  and  $\mathbf{k}$  [13]

$$\mathbf{l} = \mathbf{k} + \frac{x^{3/2}}{Gm^2} \left\{ \left( -\frac{1}{2} S_n - \frac{1}{2} \frac{\delta m}{m} \Sigma_n \right) \mathbf{n} + \left( 3S_\lambda + \frac{\delta m}{m} \Sigma_\lambda \right) \boldsymbol{\lambda} \right\}, \quad (23)$$

where  $\boldsymbol{\Sigma} = m(\mathbf{S}_2/m_2 - \mathbf{S}_1/m_1)$  as introduced in [13], while  $\delta m = m_1 - m_2$ . Further,  $(S_n, \Sigma_n)$  and  $(S_\lambda, \Sigma_\lambda)$  are the components of  $\mathbf{S}$  and  $\boldsymbol{\Sigma}$  along  $\mathbf{n}$  and  $\boldsymbol{\lambda}$ , respectively. Taking time derivative of the above equation and using equation (12a) for  $\dot{\mathbf{k}}$  gives

$$\dot{\mathbf{l}} = -2 \frac{c^3}{Gm} x^3 \left\{ \delta_1 q \chi_1 (\mathbf{s}_1 \cdot \mathbf{n}) + \frac{\delta_2}{q} \chi_2 (\mathbf{s}_2 \cdot \mathbf{n}) \right\} \boldsymbol{\lambda}. \quad (24)$$

We now compute terms that appear in the coefficient of  $\mathbf{l}$  in the expression for  $\dot{\mathbf{n}}$ , given by equation (19) using the above equation for  $\dot{\mathbf{l}}$  and equation (18c) for  $\mathbf{l}$ . They are given by

$$\begin{aligned} \sin \Phi' \frac{dt'}{dt} = \cos \Phi' \sin l' \frac{d\alpha'}{dt} = 2 \frac{c^3}{Gm} x^3 \sin \Phi' \cos \Phi' & \left\{ \delta_1 q \chi_1 (\mathbf{s}_1 \cdot \mathbf{n}) \right. \\ & \left. + \frac{\delta_2}{q} \chi_2 (\mathbf{s}_2 \cdot \mathbf{n}) \right\}. \end{aligned} \quad (25)$$

Therefore, the coefficient of  $\mathbf{l}$  in the expression for  $\dot{\mathbf{n}}$  computed using the appropriate expression for  $\dot{\mathbf{l}}$  indeed vanishes as required.

It turns out that  $\dot{\mathbf{n}}$  having components along  $\mathbf{l}$  leads to anomalous terms that contribute to  $\Phi'$  evolution at the 3PN order and this is within the consideration of higher order spin effects available in the literature. Thanks to very detailed PN computations, it should be possible, in principle, to write down a differential equation for  $\Phi'$  that incorporates the next-to-next-to-leading order spin-orbit and spin-spin interactions [20, 21, 22]. It should be noted that higher order spin-orbit and spin-spin interactions contribute to the orbital dynamics at 3.5PN and 4PN orders, respectively, for maximally spinning BH binaries. To verify the above statement we observe that the definitions  $\mathbf{v} = r \dot{\mathbf{n}}$  and  $v = r \omega$  imply that  $\omega^2 = \dot{\mathbf{n}} \cdot \dot{\mathbf{n}}$ . With the help of our equation (19) the expression for  $\omega^2$  reads

$$\omega^2 = \left( \frac{d\Phi'}{dt} + \cos \iota' \frac{d\alpha'}{dt} \right)^2 + \left( \frac{d\iota'}{dt} \sin \Phi' - \sin \iota' \cos \Phi' \frac{d\alpha'}{dt} \right)^2, \quad (26)$$

Taking the square root leads to

$$\omega = \left( \frac{d\Phi'}{dt} + \cos \iota' \frac{d\alpha'}{dt} \right) + \frac{1}{2\dot{\Phi}'} \left( \frac{d\iota'}{dt} \sin \Phi' - \sin \iota' \cos \Phi' \frac{d\alpha'}{dt} \right)^2, \quad (27)$$

where  $\dot{\Phi}'$  obviously stands for  $d\Phi'/dt$  and higher order terms that are cubic in the time derivatives of  $\iota'$  and  $\alpha'$  are neglected. Invoking the fact that  $\dot{\Phi}'$  at the Newtonian order is given by  $x^{3/2}/(Gm/c^3)$  and noting that  $d\iota'/dt$  and  $d\alpha'/dt$  have  $c^3 x^3/(Gm)$  as the common factor, we get

$$\dot{\Phi}' = \frac{c^3}{Gm} x^{3/2} \left( 1 + x^{3/2} A' + x^3 B' \right), \quad (28)$$

such that  $A'$  and  $B'$  are given by

$$A' = -\frac{\cos \iota'}{\sin \iota'} \left\{ [\delta_1 q \chi_1 (\mathbf{s}_1 \cdot \boldsymbol{\lambda}) + \frac{\delta_2}{q} \chi_2 (\mathbf{s}_2 \cdot \boldsymbol{\lambda})] \cos \Phi' + [\delta_1 q \chi_1 (\mathbf{s}_1 \cdot \mathbf{n}) + \frac{\delta_2}{q} \chi_2 (\mathbf{s}_2 \cdot \mathbf{n})] \sin \Phi' \right\}, \quad (29)$$

$$B' = -\frac{1}{2} \left\{ \delta_1 q \chi_1 (\mathbf{s}_1 \cdot \boldsymbol{\lambda}) + \frac{\delta_2}{q} \chi_2 (\mathbf{s}_2 \cdot \boldsymbol{\lambda}) \right\}^2. \quad (30)$$

These expressions mainly arise from the curly brackets present on the RHS of equations (21) and (22). It should be evident that the  $B'$  terms appear at the 3PN order while  $A'$  terms enter  $\dot{\Phi}'$  expression at the 1.5PN order. It is not very difficult to infer that these  $B'$  terms arise due to the non-vanishing  $\mathbf{l}$  component in the expression for  $\dot{\mathbf{n}}$  and therefore are unphysical in nature. This computation shows that the anomalous  $\mathbf{l}$  components in the expression for  $\dot{\mathbf{n}}$  contribute to  $\Phi'$  evolution at an order that is within the consideration of higher order spin effects available in the literature.

Let us note that we do not freely specify the two spins in a non-inertial orbital triad as usually done in the literature [16, 14]. Recall that we freely specify the two spin vectors in an inertial source frame associated with  $\mathbf{j}_0$ , namely the usual source frame, at the initial epoch. This choice allowed us to estimate the initial  $x$  and  $y$  components of  $\mathbf{k}$  in the source frame uniquely in terms of the orientations of  $\mathbf{s}_1, \mathbf{s}_2$  and other intrinsic binary parameters at the initial epoch, as given by equations (16). This is

mainly because at the initial epoch one is allowed to let  $\mathbf{j}_0$  along the  $z$ -axis without any loss of generality and thereby allowing us to impose that the  $x$  and  $y$  components of  $\mathbf{J} = \mathbf{L} + \mathbf{S}_1 + \mathbf{S}_2$  should vanish at that epoch. In contrast, it is usual to specify freely the two spins in a Cartesian coordinate system where  $\mathbf{l}$  points along the  $z$ -axis while computing the time-domain GW polarization states for inspiraling spinning compact binaries. Therefore, the following steps are required to evaluate the expressions for  $h_{+|Q}(t)$  and  $h_{\times|Q}(t)$ , given by equations (8), specified in the  $\mathbf{j}_0$ -based source frame. In the first step, the three Cartesian components of the total angular momentum at the initial epoch are computed and the two angles,  $(\theta_j, \phi_j)$ , that specify the orientation of  $\mathbf{j}_0$  in the  $\mathbf{l}$ -based Cartesian coordinate system are estimated. The second step involves rotating the  $\mathbf{j}_0$ ,  $\mathbf{l}$ ,  $\mathbf{s}_1$  and  $\mathbf{s}_2$  vectors, specified in the above  $\mathbf{l}$  frame, by the two angles  $-\theta_j$  and  $-\phi_j$ . This results in a new Cartesian coordinate system where  $\mathbf{j}_0$  points along the  $z$ -axis and  $\mathbf{l}$  is given by  $(\sin \theta_j, 0, \cos \theta_j)$ . This is the frame where one obtains the temporally evolving  $h_{+|Q}(t)$  and  $h_{\times|Q}(t)$  by simultaneously solving the Cartesian components of  $\mathbf{l}$ ,  $\mathbf{s}_1$  and  $\mathbf{s}_2$  along with the PN-accurate differential equations for  $\Phi'$  and  $x$ . Further, it is easy to note that the initial estimates for  $\theta_j$  and  $\iota$  are equal from the definitions of these two angles.

We observe that the resultant  $\mathbf{j}_0$  source frame is different from our source frame, depicted in figure 1. This is because the  $x$  and  $y$  axes of these two  $\mathbf{j}_0$ -based source frames do not usually coincide. However, it is possible to align the  $x$  and  $y$  axes of these two frames by rotating our source frame about  $\mathbf{j}_0$  such that  $\mathbf{k}$  lies in the  $x$ - $z$  plane. We have verified that the accumulated changes in  $\Phi, \alpha$  and  $\iota$  in the aLIGO frequency window are similar while evolving spinning compact binaries in these two source frames. Finally, we note that the two spins should not be freely specified in the  $\mathbf{l}$ -based orbital triad as displayed in figure 4 of [16]. This is because of the equations (38) in [16] that are required to define the unit vectors of the  $(\mathbf{e}_1, \mathbf{e}_2, \mathbf{e}_3 \equiv \mathbf{l})$  triad. It is easy to infer that the definition of  $\mathbf{e}_1 \propto \mathbf{l} \times \mathbf{j}_0$  implies that  $\mathbf{j}_0 \cdot \mathbf{e}_1 \equiv 0$ . However, this dot product will not vanish if one freely specifies the two spins in the above orbital triad and evaluate  $\mathbf{j}_0 \cdot \mathbf{e}_1$  by computing  $\mathbf{J}$  at the initial epoch. This anomalous feature is the main reason for stating that the two spins should not be freely specified at the initial epoch in the above orbital triad.

A consequence of invoking  $\mathbf{k}$  to specify the binary orbit is the appearance of new 1.5PN contributions to the amplitudes of  $h_+$  and  $h_\times$  in addition to what is provided by equations (A2) and (A3) in [14]. These additional amplitude corrections to GW polarization states arise mainly due to the fact that the component of  $\mathbf{v}$  along  $\mathbf{k}$  is of 1.5PN order and enter expressions for  $h_+$  and  $h_\times$  through the dot products  $(\mathbf{p} \cdot \mathbf{v})(\mathbf{q} \cdot \mathbf{v})$  and  $(\mathbf{p} \cdot \mathbf{v})^2 - (\mathbf{q} \cdot \mathbf{v})^2$  present in equations (4).

The resulting 1.5PN order amplitude corrections to  $h_+$  and  $h_\times$  read

$$\begin{aligned}
h_+ \Big|_{1.5\text{PN}} = \frac{G\mu}{c^4 R'} \frac{Gm}{2c^3 \sqrt{x}} \Big\{ & \left[ (\cos \iota + 1) (1 + C_\theta^2) \sin \iota \sin(2\alpha + 2\Phi) \right. \\
& - (\cos \iota - 1) (1 + C_\theta^2) \sin \iota \sin(2\alpha - 2\Phi) \\
& - (-4 \cos^2 \iota + 2 \cos \iota + 2) S_\theta C_\theta \sin(\alpha - 2\Phi) \\
& + (-2 \cos \iota - 4 \cos^2 \iota + 2) S_\theta C_\theta \sin(\alpha + 2\Phi) \\
& - (2 + 2 C_\theta^2) \sin \iota \sin(2\alpha) + 4 C_\theta S_\theta \sin \alpha \cos \iota \\
& + (-6 + 6 C_\theta^2) \cos \iota \sin \iota \sin(2\Phi) \Big] i + \left[ (-4 + 8 \cos^2 \iota) \sin \iota S_\theta C_\theta \cos \alpha \right. \\
& + (2 \cos \iota + 4 \cos^2 \iota - 2) \sin \iota S_\theta C_\theta \cos(\alpha + 2\Phi) \\
& + (\cos^3 \iota + \cos^2 \iota - \cos \iota - 1) (1 + C_\theta^2) \cos(2\alpha + 2\Phi) \\
& + (-2 + 4 \cos^2 \iota - 2 \cos \iota) S_\theta C_\theta \sin \iota \cos(\alpha - 2\Phi) \\
& + (\cos^3 \iota - \cos^2 \iota - \cos \iota + 1) (1 + C_\theta^2) \cos(2\alpha - 2\Phi) \\
& + (-6 \cos^2 \iota + 6) (1 - C_\theta^2) \cos \iota \cos(2\Phi) \\
& + (-6 + 2 \cos(2\alpha) + 2 C_\theta^2 \cos(2\alpha) + 6 C_\theta^2) \cos^3 \iota \\
& \left. + (-2 C_\theta^2 \cos(2\alpha) - 6 C_\theta^2 + 6 - 2 \cos(2\alpha)) \cos \iota \right] \dot{\alpha} \Big\}, \tag{31a}
\end{aligned}$$

$$\begin{aligned}
h_\times \Big|_{1.5\text{PN}} = \frac{G\mu}{c^4 R'} \frac{Gm}{c^3 \sqrt{x}} \Big\{ & \left[ (2 \cos^2 \iota + \cos \iota - 1) S_\theta \cos(\alpha + 2\Phi) \right. \\
& + (-\cos \iota - 1) C_\theta \sin \iota \cos(2\alpha + 2\Phi) + (\cos \iota - 2 \cos^2 \iota + 1) S_\theta \cos(\alpha - 2\Phi) \\
& + (\cos \iota - 1) C_\theta \sin \iota \cos(2\alpha - 2\Phi) - 2 S_\theta \cos \alpha \cos \iota + 2 C_\theta \sin \iota \cos(2\alpha) \Big] i \\
& + \left[ (\cos^3 \iota - \cos \iota + \cos^2 \iota - 1) C_\theta \sin(2\Phi + 2\alpha) \right. \\
& - (\cos \iota - 2 \cos^2 \iota + 1) S_\theta \sin \iota \sin(\alpha - 2\Phi) \\
& - (-\cos^3 \iota + \cos^2 \iota + \cos \iota - 1) C_\theta \sin(2\alpha - 2\Phi) \\
& + (2 \cos^2 \iota + \cos \iota - 1) S_\theta \sin \iota \sin(\alpha + 2\Phi) + (4 \cos^2 \iota - 2) S_\theta \sin \iota \sin \alpha \\
& \left. - 2 C_\theta \cos \iota \sin(2\alpha) + 2 C_\theta \cos^3 \iota \sin(2\alpha) \right] \dot{\alpha} \Big\}, \tag{31b}
\end{aligned}$$

where  $x$  equals the square of the invariant velocity employed in [14]. Therefore, the fully 1.5PN order amplitude corrected  $h_+$  and  $h_\times$  for spinning compact binaries in quasi-circular orbits, specified by  $\mathbf{L}$ , are provided by equations (A2) and (A3) in [14] along with above two 1.5PN order contributions. This requires that the  $\iota$  and  $\alpha$  variables of [14] that appear in their equations (A2) and (A3) describe  $\mathbf{k}$  rather than  $\mathbf{l}$ . In contrast, the equations (A2) and (A3) in [14] indeed provide the fully 1.5PN order amplitude corrected  $h_+$  and  $h_\times$  for spinning compact binaries while invoking  $\mathbf{l}$  to describe the quasi-circular orbits. Let us state again that it will be desirable to involve equation (24) to evolve  $\mathbf{l}$  due to the earlier discussions. It will be interesting to probe the influence of these amplitude corrections to the parameter estimation accuracies. We observe that the combined effects of spin-precession, subdominant

harmonics and amplitude modulations indeed improved the parameter estimation accuracies of massive BH binaries that LISA should observe [28]. Additionally, our expressions for  $h_{+,\times}(t)$  should be appealing while constructing amplitude corrected spinning binary templates invoking the Effective One Body (EOB) approach [29]. This is because the EOB Hamiltonian approach naturally employs  $\mathbf{L}$  to describe orbits.

In what follows we explore, motivated purely by few theoretical considerations, if it is essential to employ an orbital-like frequency  $\omega_{\text{orb}}$  while employing the  $(\mathbf{n}, \boldsymbol{\xi}, \mathbf{k})$  frame to perform GW phasing for spinning compact binaries. Let us emphasize that the next section is not an alternative to what is detailed in this section and further investigations will be required to extract implications of these theoretical considerations.

### 3. Another plausible approach for GW phasing while using $\mathbf{L}$ to specify binary orbits

We begin by listing the theoretical considerations that prompted us to explore alternatives to an orbital-like frequency  $\omega_{\text{orb}}$  while computing inspiral templates for spinning compact binaries. We note that the orbital-like frequency  $\omega_{\text{orb}}$  naturally arises in the  $(\mathbf{n}, \boldsymbol{\lambda}, \mathbf{l})$  frame leading to the following PN independent expressions for binaries in circular orbits:  $\mathbf{v} = r \omega_{\text{orb}} \boldsymbol{\lambda}$  and  $\omega_{\text{orb}} \equiv v/r$ . These expressions allow us to write  $\omega_{\text{orb}} \equiv \dot{\mathbf{n}} \cdot \boldsymbol{\lambda}$  which leads to the usually employed prescription to model  $\Phi'(t)$ , namely  $\omega_{\text{orb}} = \dot{\Phi}' + \cos \iota' \dot{\alpha}'$  [9, 14]. Therefore, the phase evolution  $\Phi'(t)$  becomes

$$\Phi'(t) = \int_0^t [\omega_{\text{orb}}(t') - \cos \iota'(t') \dot{\alpha}'(t')] dt', \quad (32)$$

where the temporal evolution for  $\omega_{\text{orb}}$  arises only due to reactive evolution of  $x$ , given by equation (15), while temporal evolutions for  $\iota'$  and  $\alpha'$  are generated by the combined influences of both conservative and reactive dynamics. However, the expression that complements  $\mathbf{v} = r \omega_{\text{orb}} \boldsymbol{\lambda}$  in our frame involves the conjugate momentum  $\mathbf{p} = \mathbf{p}_{\perp} \boldsymbol{\xi}$  where  $\mathbf{p}_{\perp}^2 = (\mathbf{n} \times \mathbf{p})^2$  and therefore will not involve any specific orbital frequency [23]. The situation gets a bit more complicated due to the absence of Keplerian type parametric solution for the binaries in eccentric orbits [23]. We recall that such a parametric solution is useful to define the orbital frequency for non-spinning compact binaries in both circular and eccentric orbits [30, 31]. Finally, as noted earlier,  $\int \omega_{\text{orb}}(t') dt'$  (and its multiples) can provide GW phase evolutions for spinning binaries only when orbital inclinations are tiny so that one may neglect  $\iota$  expanded amplitude corrections to  $h_+$  and  $h_{\times}$  [14]. This is because in such a limit amplitude corrected GW polarization states can be expressed in terms of  $\sin \psi$ ,  $\cos \psi$  and their higher harmonics like  $\sin 2\psi$ ,  $\cos 2\psi$ ,  $\cos 3\psi$ , ... where  $\psi = \Phi + \alpha$ . However, in our approach orbital inclinations are usually not very tiny even at the initial epoch.

Let us begin by describing, in detail, the point involving Keplerian type parametric solution as there exists an attempt to incorrectly define  $\omega_{\text{orb}}$  for spinning binaries in eccentric orbits [32]. Recall that it is possible to define a gauge invariant orbital frequency  $\omega_{\text{orb}}$  for both eccentric (and circular) binaries with non-spinning components as noted in [30, 31]. This orbital frequency, defined as  $\omega_{\text{orb}} = n(1+k)$ , requires  $n$  and  $k$  which are the only two gauge invariant quantities of the orbital dynamics if expressed in terms of  $\epsilon = (-2E/\mu c^2)$  where  $E$  is the conserved orbital energy. These two gauge invariant quantities are associated with the radial and angular

part of Keplerian type parametric solution to the underlying conservative orbital dynamics (the Keplerian type parametric solution exists to 3PN order for eccentric binaries with non-spinning components [33]). The above orbital frequency allows one to have orbital phase varying linearly in time with certain additional periodic variations that vanish in the circular limit of eccentric binaries. In other words,  $\phi(t) = \omega_{\text{orb}} \times (t - t_0) + W(l, e_t) \equiv n \times (1 + k) \times (t - t_0) + W(l, e_t)$ , where  $W(l, e_t)$  is periodic and vanishes when eccentricity  $e_t$  goes to zero and  $l$  is defined as  $l = n(t - t_0)$  (see equations (2.6)-(2.8) in [31]). Therefore, it is natural to invoke  $\omega_{\text{orb}}$  to do GW phasing for non-spinning compact binaries moving in eccentric orbits and to explore numerical relativity and GW data analysis implications as pursued in [34, 35]. However, it is not possible to write down a similar expression for  $\Phi$  in terms of  $\omega_{\text{orb}}$  and  $W$  while considering spinning compact binaries in eccentric orbits. This is because the conservative PN dynamics of spinning compact binaries that includes the effects of dominant order spin-orbit interactions does not admit a Keplerian type parametric solution in its angular sector [23]. This can be attributed to the non-integrable nature of the angular part of the associated conservative orbital dynamics. In the absence of any naturally occurring orbital frequency  $\omega_{\text{orb}}$  in terms of  $n$  and  $k$ , [23] invoked  $\epsilon$  as the PN expansion parameter in the place of  $x = (Gm\omega_{\text{orb}}/c^3)^{(2/3)}$ . This forced [23] to invoke the far-zone energy flux to directly incorporate the effects of radiation reaction while providing an approach to compute  $h_{+, \times}(t)$  for such binaries.

It may be useful to note that [32] obtained an incorrect orbital frequency by constructing an unphysical precessing frame to accommodate the relation  $\dot{\Phi}' = \omega_{\text{orb}} - \cos i' \dot{\alpha}'$ , where  $\omega_{\text{orb}} = d\phi/dt$  such that the azimuthal phase  $\phi$  follows above mentioned Keplerian type parametric solution. It was argued in [32] that the azimuthal phase of precessing spinning compact binaries in eccentric orbits admits a Keplerian type parametric solution in a non-inertial frame that follows the precessing orbital plane, defined by  $\mathbf{L}_N$ . This is possible if the orbital velocity in the precessing non-inertial frame can be written as  $v_{\text{prec}}^2 = \dot{r}^2 + r^2 \dot{\phi}^2$ . A careful computation revealed that the expression for  $v_{\text{prec}}^2$  is more complicated for precessing binaries as evident from equations (15), (18) and (19) in [23]. Moreover, the appropriate equation for  $\dot{\phi}$  is coupled with the longitudinal motion, as clear from equations (13) in [23]. This makes it impossible to have Keplerian type parametric solution for the angular part of orbital dynamics for such binaries. In the absence of any naturally occurring orbital frequency  $\omega_{\text{orb}}$ , definable from a Keplerian type parametric solution, [23] employed scaled orbital energy as their PN expansion parameter in the place of scaled orbital frequency. This requires us to invoke the far-zone orbital energy to incorporate effects of inspiral as done in the TaylorEt approximant. The present approach provides the circular limit of what is detailed in [23] while making sure that the equation for  $\dot{\Phi}'$  is gauge-invariant. It may be possible to provide following reason for the absence of a physical orbital frequency for our binaries similar to what is pursued in the non-spinning binaries. It turns out that Keplerian type parametric solution to spinning compact binaries in eccentric orbits exists in a precessing frame, similar to the one given by equations (38) in [16], only in two special cases for binary dynamics under consideration [26]. These special cases are i) binary components have equal mass and ii) only one component is spinning and for these two cases the  $z$  component of  $\mathbf{L}$  is conserved as detailed in [26]. The existence of such a parametric solution allows one to define a physical orbital frequency  $\omega_{\text{orb}} = n(1 + k)$  with the help of equations (4.20) and (4.30) in [26]. However, the  $z$  component of  $\mathbf{L}$  is not conserved in our binaries



as evident from our equation for  $\dot{\mathbf{k}}$  making the angular part non-integrable and it again leads to the absence of a Keplerian type parametric solution. We would like to note that a recent computation provided a Keplerian type parametric solution for spinning compact binaries in eccentric orbits having their spins aligned or anti-aligned with  $\mathbf{L}$ , while incorporating higher order spin-orbit and spin-spin interactions [36]. Additionally, another recent investigation reveals that it is possible to tackle the non-integrable spin-orbit dynamics with the help of certain Lie series transformation [37]. This approach obtained an approximative solution for the spinning binary dynamics in circular orbits that included the next-to-leading-order spin-orbit interactions while expanding  $\eta$  around its equal mass value, namely  $\eta = 0.25$ .

Further, let us clarify that it is difficult to define a frame where  $\int \omega_{\text{orb}}(t') dt'$  can provide GW phase evolution for spinning compact binaries. This is demonstrated by showing that in the precessing frame  $(\hat{\mathbf{x}}_{\text{L}}, \hat{\mathbf{y}}_{\text{L}}, \mathbf{l})$  of [14] it is not possible to have  $d\Phi'/dt = \omega$  such that the adiabatic condition for a sequence of circular orbits reads  $\dot{\mathbf{n}} \equiv \omega \boldsymbol{\lambda}$ . This is rather incompatible with the conclusion present in the Appendix B of [16] as the orbital triad  $(\mathbf{e}_1, \mathbf{e}_2, \mathbf{l})$  appearing in the above Appendix is identical to the above triad as evident by comparing equations (2.9) and (2.10) of [14] with equations (B1) of [16]. We begin by writing our equation (19) for  $\dot{\mathbf{n}}$  as

$$\dot{\mathbf{n}} = \dot{\Phi}' \boldsymbol{\lambda} + \left\{ 2 \frac{c^3}{Gm} x^3 \sin \Phi' \cot \iota' \left( \delta_1 q \chi_1 (\mathbf{s}_1 \cdot \mathbf{n}) + \frac{\delta_2}{q} \chi_2 (\mathbf{s}_2 \cdot \mathbf{n}) \right) \mathbf{l} \right\} \times \mathbf{n}. \quad (33)$$

A causal comparison with equation (B2) of [16] reveals that the vectorial quantity in the curly bracket can be identified with their  $\boldsymbol{\Omega}_e$ . Interestingly in our case it points along  $\mathbf{l}$ , provided we use the correct equation for  $d\mathbf{l}/dt$ , namely our equation (24). This equation may be written as

$$\dot{\mathbf{l}} = \left\{ 2 \frac{c^3}{Gm} x^3 \left( \delta_1 q \chi_1 (\mathbf{s}_1 \cdot \mathbf{n}) + \frac{\delta_2}{q} \chi_2 (\mathbf{s}_2 \cdot \mathbf{n}) \right) \mathbf{n} \right\} \times \mathbf{l}, \quad (34)$$

and we observe that the vectorial quantity in the above curly bracket is indeed  $\propto \mathbf{n}$  as required by the equations (B4) and (B5) in [16]. However, a close inspection reveals that the curly brackets in the above two equations, namely equations (33) and (34), are not identical and therefore,  $\dot{\Phi}'$ , appearing in equation (33), can not be equated to an orbital frequency  $\omega$  required by the adiabatic condition :  $\dot{\mathbf{n}} \equiv \omega \boldsymbol{\lambda}$ . It will be interesting to explore the consequences of these observations.

These observations prompted us to use  $\epsilon$  to perform GW phasing so that the effects of GW damping can also be incorporated directly with the help of PN-accurate far-zone energy flux as done in [23]. Therefore, the present GW phasing approach may be treated as the straightforward circular limit of the prescription, detailed in [23], to compute temporally evolving GW polarization states for spinning compact binaries in inspiraling eccentric orbits. The fact that we are going to invoke  $\epsilon$  to do GW phasing makes it similar to Taylor-Et approximant, introduced in [24] for non-spinning compact binaries. This approximant was found to be incompatible with various other approximants that provided inspiral templates for non-spinning compact binaries and therefore undesirable from the GW data analysis point of view [25]. However, the Taylor-Et approximant may be interesting while dealing with spinning compact binaries as evident from figure 3 in [38]. This paper compared the accumulated phase difference arising from numerical relativity and various PN approximants over the ten cycles before the scaled GW frequency reached 0.1. The comparisons were done

for equal-mass binaries whose black holes have equal spins oriented parallel to the orbital angular momentum. It was noted that at the 2.5PN order (the highest PN order at which all terms are known) the TaylorEt approximant provided the least accumulated phase disagreements especially for high spin configurations. Therefore, further investigations will be required to probe physical implications of our present prescription, based purely on above mentioned theoretical arguments.

Let us first obtain the differential equation for  $\Phi$  in this approach and it also requires the PN-accurate relation  $v/r = \dot{\Phi} + \dot{\alpha} \cos \iota$  that originates from equation (6b). We invoke the equations (6.1) and (6.5) in [13] to obtain  $v/r$  first in terms of  $Gm/c^2 r$  and then in terms of  $\epsilon$  to the 2PN order. We employ such a PN-accurate expression for  $v/r$  to obtain the following equation for  $\dot{\Phi}$ :

$$\begin{aligned} \dot{\Phi} = \frac{c^3}{Gm} \epsilon^{3/2} \left\{ 1 + \epsilon \left( \frac{9}{8} + \frac{\eta}{8} \right) - \epsilon^{3/2} \left[ (3 + X_1) X_1 \chi_1 (\mathbf{s}_1 \cdot \mathbf{k}) \right. \right. \\ \left. \left. + (3 + X_2) X_2 \chi_2 (\mathbf{s}_2 \cdot \mathbf{k}) \right] + \epsilon^2 \left( \frac{11}{128} \eta^2 - \frac{201}{64} \eta + \frac{891}{128} \right) \right\} - \cos \iota \dot{\alpha}. \end{aligned} \quad (35)$$

This is clearly equivalent to equation (11) for  $\dot{\Phi}$  while employing PN-accurate expression for  $\omega_{\text{orb}}$  in terms of  $\epsilon$  as expected.

The other aspects of the conservative dynamics, relevant for GW phasing, are provided by the following precessional equations for  $\mathbf{k}$ ,  $\mathbf{s}_1$  and  $\mathbf{s}_2$

$$\dot{\mathbf{k}} = \frac{c^3}{Gm} \epsilon^3 \left\{ \delta_1 q \chi_1 (\mathbf{s}_1 \times \mathbf{k}) + \frac{\delta_2}{q} \chi_2 (\mathbf{s}_2 \times \mathbf{k}) \right\}, \quad (36a)$$

$$\dot{\mathbf{s}}_1 = \frac{c^3}{Gm} \epsilon^{5/2} \delta_1 (\mathbf{k} \times \mathbf{s}_1), \quad (36b)$$

$$\dot{\mathbf{s}}_2 = \frac{c^3}{Gm} \epsilon^{5/2} \delta_2 (\mathbf{k} \times \mathbf{s}_2). \quad (36c)$$

These equations are clearly obtained from their  $x$  counterparts by simply substituting  $x$  by  $\epsilon$  as at the Newtonian order  $x = \epsilon$ . Clearly, the above equations along with equation (35) provide how the Eulerian angles  $\Phi$ ,  $\alpha$  and  $\iota$ , appearing in the expressions for  $h_{+, \times}(t)$ , vary under the precessional and conservative dynamics in the  $\epsilon$ -approach. The effect of gravitational radiation reaction is incorporated by allowing  $\epsilon$  to vary according to

$$\begin{aligned} \frac{d\epsilon}{dt} = \frac{64}{5} \frac{c^3}{Gm} \eta \epsilon^5 \left\{ 1 + \epsilon \left( \frac{13}{336} - \frac{5}{2} \eta \right) + 4\pi \epsilon^{3/2} \right. \\ \left. + \frac{\epsilon^{3/2}}{12} \left[ (-328 X_1 + 135 \sqrt{1-4\eta}) X_1 \chi_1 (\mathbf{s}_1 \cdot \mathbf{k}) \right. \right. \\ \left. \left. - (328 X_2 + 135 \sqrt{1-4\eta}) X_2 \chi_2 (\mathbf{s}_2 \cdot \mathbf{k}) \right] \right. \\ \left. + \epsilon^2 \left( \frac{5}{2} \eta^2 - \frac{12017}{2016} + \frac{117857}{18144} \right) \right\}. \end{aligned} \quad (37)$$

The above expression may be extracted from the 2PN accurate expressions for the far-zone energy flux and the conserved energy expressed in terms of  $x$ , given by equations (6.4), (6.6) and (7.11) in [13]. It should be obvious that we need to

solve together equations (35), (36) and (37) numerically to obtain how  $\Phi, \iota, \alpha$  and  $\dot{\Phi}$  temporally vary in the present approach, while employing Cartesian components of equations (36). In what follows we sketch how we specify various required initial values.

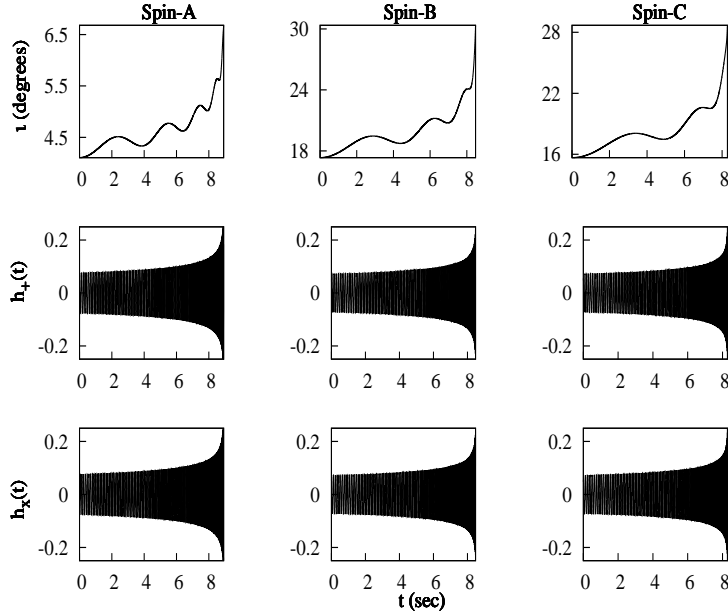


**Figure 4.** Plots, similar to figure 2, displaying temporally evolving  $\iota(t)$ , scaled  $h_{+|\mathcal{Q}}(t)$  and  $h_{\times|\mathcal{Q}}(t)$  for maximally spinning compact binaries ( $q = 1, m = 50M_{\odot}$ ) while using  $\epsilon$  as the PN expansion parameter. A visual comparison with figure 2 fails to provide any noticeable differences.

The initial values for the Cartesian components of  $\mathbf{s}_1$  and  $\mathbf{s}_2$  in the inertial frame are provided with the help of equations (14) by choosing various possible values for  $\theta_1, \phi_1, \theta_2$  and  $\phi_2$  as expected. The initial values for  $k_x$  and  $k_y$  are also obtained with the help of equations (16) and we let  $\Phi = 0$  at the initial epoch. The bounding values for the numerical integration, namely the initial and final values of  $\epsilon$ , are obtained by numerically inverting the following 2PN accurate expression for  $x$  in terms of  $\epsilon$

$$x = \epsilon \left\{ 1 + \epsilon \left( \frac{\eta}{12} + \frac{3}{4} \right) - \epsilon^{3/2} \left[ \left( 2 - \frac{2}{3} X_1 \right) X_1 \chi_1 (\mathbf{s}_1 \cdot \mathbf{k}) + \left( 2 - \frac{2}{3} X_2 \right) X_2 \chi_2 (\mathbf{s}_2 \cdot \mathbf{k}) \right] + \epsilon^2 \left( \frac{\eta^2}{18} - \frac{17}{8} \eta + \frac{9}{2} \right) \right\}. \quad (38)$$

Following the previous section, the lower limit for  $\epsilon$  corresponds to  $x = 2.9 \times 10^{-4} (m \omega_0)^{2/3}$  while the terminating value of  $\epsilon$  is obtained by numerically evaluating the above equation for  $x$  at every epoch and making sure that  $x$  never crosses the usual final value of  $1/6$ . We are now in a position to obtain plots, similar to figures 2 and 3, depicting temporal evolutions of  $\iota(t)$  and scaled  $h_{+, \times|\mathcal{Q}}(t)$  while using  $\epsilon$  as the PN expansion parameter and these are displayed in figures 4 and 5.

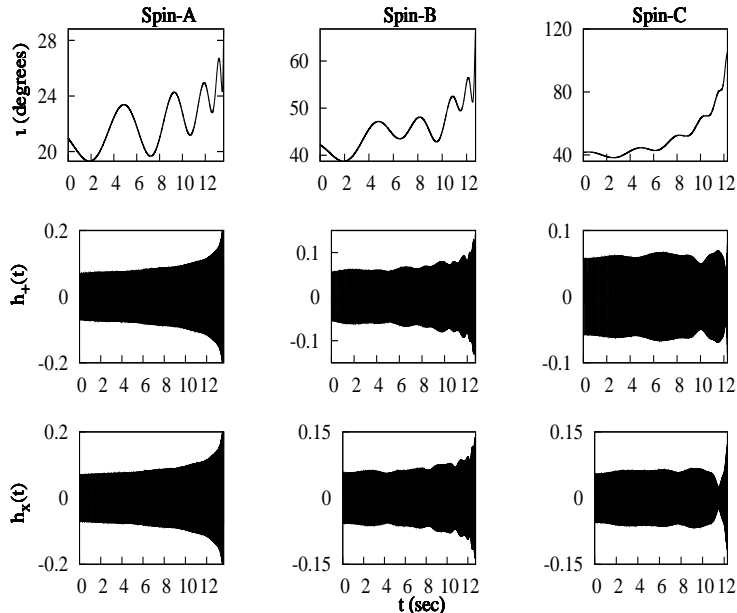


**Figure 5.** A set of plots, similar to those displayed in figure 3, while using  $\epsilon$  as the PN expansion parameter for unequal mass maximally spinning compact binaries ( $q = 4, m = 50M_\odot$ ).

A visual comparison between the plots in figure 2 and 4 for  $q = 1$  binaries and relevant plots in figure 3 and 5 for  $q = 4$  binaries reveals no significant differences between the two approaches. However, plots for the difference in  $\Phi$  evolution while invoking our two prescriptions show noticeable differences in their late time phase evolutions. The plots in figure 6 show that the  $\Phi$  differences can be large. For example, we find  $\Delta\Phi \sim 40$  radians for a binary with  $q = 4$  in Spin-C configuration. It will be desirable to probe the differences in GW phase evolutions described by Numerical Relativity and our PN accurate prescriptions for equal and unequal mass precessing binaries after extending the present approaches to include higher order precessional and reactive dynamics. Let us note that such a comparison already exists for equal mass BH binaries having their spins aligned to orbital angular momentum while invoking both  $x$  and  $\epsilon$  to obtain GW phase evolutions during late stages of inspiral [38]. These discussions should also be useful to probe any plausible data analysis implications even though non-spinning version of the  $\epsilon$ -approach was found to be undesirable in [25].

#### 4. Discussion

We presented a prescription to compute the time-domain GW polarization states associated with spinning compact binaries inspiraling along quasi-circular orbits. We invoked the orbital angular momentum  $\mathbf{L}$  rather than its Newtonian version  $\mathbf{L}_N$  to describe the binary orbits. Additionally, we freely specified the two spins in an inertial frame associated with the initial direction of the total angular momentum  $\mathbf{j}_0$  at the initial epoch. In this paper, the precessional dynamics is governed by the

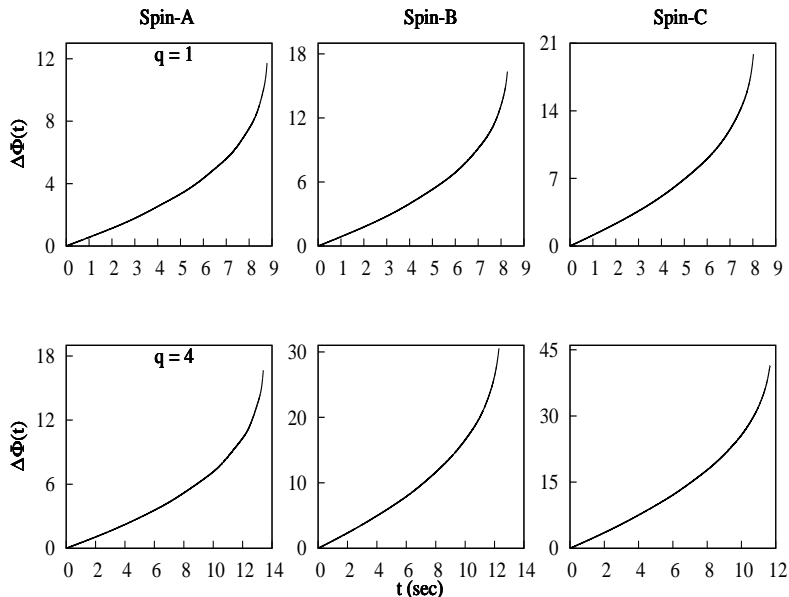


**Figure 6.** The differences in the orbital phase evolution under the  $x$  and  $\epsilon$  approaches. We consider two sets of binaries having  $q = 1$  (upper panel) and  $q = 4$  (lower panel) for the earlier discussed three initial spin configurations: Spin-A (left panel), Spin-B (middle panel) and Spin-C (right panel).

leading order spin-orbit coupling while allowing both compact objects to spin and the inspiral dynamics is fully 2PN accurate including the dominant order spin-orbit contributions to  $dx/dt$ . We also probed the consequence of employing the precessional equation appropriate for  $\mathbf{L}$  to numerically evolve  $\mathbf{L}_N$  and showed that the 1.5PN order component of orbital velocity  $\mathbf{v}$  along  $\mathbf{L}_N$  will not, in general, vanish. We pointed out that this undesirable feature creates anomalous terms in the phase evolution that enter the dynamics at the relative 3PN order. However, our GW phase evolution is identical to what is provided in [14] as both these investigations incorporate only the dominant 1.5PN accurate spin-orbit effects. The fact that we employ  $\mathbf{L}$  to describe the binary orbits implies that the orbital velocity can have non-vanishing components along  $\mathbf{L}$ . This leads to additional 1.5PN order amplitude corrections to GW polarization states compared the 1.5PN accurate amplitude corrected expressions for  $h_+$  and  $h_\times$ , available in [14] that employ  $\mathbf{L}_N$  to describe the binary orbits. We pointed out that by adding these 1.5PN order amplitude corrections to equations (A2) and (A3) in [14] should result in the fully 1.5PN order amplitude corrected  $h_+$  and  $h_\times$  for spinning compact binaries in quasi-circular orbits described by  $\mathbf{L}$ . In comparison, the equations (A2) and (A3) in [14] provide the fully 1.5PN order amplitude corrected  $h_+$  and  $h_\times$  for spinning compact binaries in quasi-circular orbits characterized by  $\mathbf{L}_N$ .

Influenced by few purely theoretical considerations, we provided a plausible prescription to perform GW phasing that requires us to employ far-zone energy flux to implement directly the effects of gravitational radiation reaction. The theoretical considerations include an efficient phasing prescription for spinning compact binaries inspiraling along PN accurate eccentric orbits [23]. Additional considerations include

the fact that the orbital-like frequency  $\omega_{\text{orb}}$  naturally appears in the  $\mathbf{l}$  based triad, defined using  $\mathbf{l}$  and  $\mathbf{n}$  and that  $\int \omega_{\text{orb}}(t') dt'$  and its multiples provide GW phase evolutions for binaries having tiny orbital inclinations. Further investigations will be required to probe the physical implications of our  $\epsilon$  prescription as its non-spinning version found to be undesirable in [25].

It will be interesting to compare our numerical approach to describe dynamics of spinning compact binaries with the approximate solution, provided in [37], that invoked similar angular variables. We also plan to compare GW phase evolutions under our two prescriptions with those obtained from accurate NR simulations [39].

## Acknowledgments

We thank Guillaume Faye and Gerhard Schäfer for detailed discussions and encouragements. We are grateful to P. Ajith, B. Sathyaprakash and N. Mazumder for clarifying the implementation of  $h_{+, \times}(t)$  in the LSC Algorithm Library Suite. The algebraic computations, appearing in this paper, were performed using MAPLE and MATHEMATICA.

## References

- [1] Harry G M (the LIGO Scientific Collaboration) 2010 *Class. Quantum Grav.* **27** 084006
- [2] Accadia T et al (The Virgo Collaboration) 2011 Status of the Virgo project *Class. Quantum Grav.* **28** 114002; The Virgo Collaboration 2009 note VIR-027A-09 <https://tds.ego-gw.it/itf/tds/file.php?callFile=VIR-0027A-09.pdf>
- [3] Somiya K (the KAGRA collaboration) 2012 *Class. Quantum Grav.* **29** 124007
- [4] Cutler C, Finn L S, Poisson E and Sussman G J 1993 *Phys. Rev. D* **47** 1511
- [5] Numerous authors have worked on the post-Newtonian accurate binary dynamics involving spinning bodies of comparable mass. For a recent review, see Blanchet L, *Gravitational Radiation from Post-Newtonian Sources and Inspiralling Compact Binaries*, 2002 *Living Rev. Rel.* **5** 3
- [6] Blanchet L, Iyer B R and Joquet B 2002 *Phys. Rev. D* **65** 064005
- [7] Blanchet L, Damour T, Esposito-Farèse G and Iyer B R 2004 *Phys. Rev. Lett.* **93** 091101
- [8] Blanchet L, Faye G, Iyer B R and Sinha S 2008 *Class. Quantum Grav.* **25** 165003
- [9] Kidder L 1995 *Phys. Rev. D* **52** 821
- [10] Damour T and Schäfer G 1988 *Nuovo Cimento B* **101** 127
- [11] Lattimer J M and Prakash M 2001 *Astrophys. J.* **550** 426
- [12] Faye G, Blanchet L and Buonanno A 2006 *Phys. Rev. D* **74** 104033
- [13] Blanchet L, Buonanno A and Faye G 2006 *Phys. Rev. D* **74** 104034
- [14] Arun K G, Buonanno A, Faye G and Ochsner E 2009 *Phys. Rev. D* **79** 104023
- [15] Buonanno A, Faye G and Hinderer T 2013 *Phys. Rev. D* **87** 044009
- [16] Buonanno A, Chen Y and Vallisneri M 2003 *Phys. Rev. D* **67** 104025
- [17] Apostolatos T A, Cutler C, Sussman G J and Thorne K 1994 *Phys. Rev. D* **49** 6274
- [18] Arnowitt R L, Deser S and Misner C W 2008 *Gen. Rel. Grav.* **40** 1997-2027
- [19] Steinhoff J, Schäfer G and Hergt S 2008 *ADM Phys. Rev. D* **77** 104018
- [20] Marsat S, Bohe A, Faye G and Blanchet L 2013 *Class. Quantum Grav.* **30** 055007
- [21] Hartung J and Steinhoff J 2011 *Annalen der Physik* **523** 783, arXiv:1104.3079 [gr-qc]
- [22] Hartung J, Steinhoff J and Schäfer G 2013 *Annalen der Physik* **525** 359, arXiv:1302.6723 [gr-qc]
- [23] Gopakumar A and Schäfer G 2011 *Phys. Rev. D* **84** 124007
- [24] Gopakumar A, arXiv:0712.3236
- [25] Buonanno A, Iyer B R, Ochsner E, Pan Y and Sathyaprakash B S 2009 *Phys. Rev. D* **80** 084043
- [26] Königsdörffer C and Gopakumar A 2005 *Phys. Rev. D* **71** 024039
- [27] Barker B and O'Connell R 1975 *Phys. Rev. D* **12** 329
- [28] Klein A, Jetzer P and Sereno M 2009 *Phys. Rev. D* **80** 064027
- [29] Taracchini A et al, arXiv:1311.2544
- [30] Blanchet L, Damour T and Iyer B 1995 *Phys. Rev. D* **51** 5360
- [31] Arun K G, Blanchet L, Iyer B R and Qusailah M S S 2008 *Phys. Rev. D* **77** 064034; **77** 064035

- [32] Cornish N J and Key J S 2010 *Phys. Rev. D* **82** 044028
- [33] Memmesheimer R M, Gopakumar A and Schäfer G 2004 *Phys. Rev. D* **70** 104011
- [34] Hinder I, Herrmann F, Laguna P and Shoemaker D 2010 *Phys. Rev. D* **82** 024033
- [35] Brown D A and Zimmerman P J 2010 *Phys. Rev. D* **81** 024007
- [36] Tessmer M, Hartung J and Schäfer G 2013 *Class. Quantum Grav.* **30** 015007
- [37] Tessmer M, Steinhff J and Schäfer G 2013 *Phys. Rev. D* **87** 064035
- [38] Hannam M, Husa S, Brüggmann B and Gopakumar A 2008 *Phys. Rev. D* **78** 104007
- [39] Mroue A H, Scheel M A, Szilagyi B, Pfeiffer H P, Boyle M et al, arXiv:1304.6077